Understanding the Thermochemical Reactions of Lithium and Carbonate Electrolytes at Elevated Temperatures

Juyoung Oh and Ming Tang
Rice University
6100 Main St, Houston, TX 77005, USA

1 Introduction

Lithium metal batteries (LMBs), utilizing lithium metal as the anode, are considered promising candidates for next-generation energy storage systems due to their exceptional theoretical capacity (3,860 mAh/g) compared to lithium-ion batteries (LIB, 372 mAh/g) [1]. However, their practical implementation is hindered by critical safety concerns, particularly thermal runaway (TR). The high reactivity of Li, dendrite growth, and the unstable solid electrolyte interphase (SEI) on the Li surface are key contributors to these safety challenges in LMBs, leading to both electrochemical performance degradation and the onset of TR [2]. Addressing these challenges necessitates a fundamental understanding of the thermochemical interactions between the Li metal anode and the electrolyte−two components that are directly implicated in triggering TR in LMB systems.

To elucidate the chemical reactions between Li and electrolytes, various experimental techniques have been employed, including nuclear magnetic resonance (NMR), X-ray photoelectron spectroscopy (XPS), X-ray diffraction (XRD), gas chromatography-mass spectrometry (GC-MS), differential scanning calorimetry (DSC), thermogravimetry analysis (TGA), and accelerating rate calorimeter (ARC) [3-5]. These techniques have provided valuable insights into the complex reaction mechanisms within Li-electrolyte systems. However, precise mechanisms and the identification of the primary reactants and products responsible for significant heat release remain elusive. Moreover, the specific chemical pathways and trigger reactions in Li-electrolyte systems, particularly involving carbonate electrolytes, are insufficiently understood. There is also ongoing debate about the chemical reactions, including thermal decomposition, electrolyte boiling, and Li reduction. Thus, it is crucial to quantitatively and qualitatively identify the specific reactants and products involved in these reactions at elevated temperatures.

This study investigates the fundamental reaction mechanisms between Li metal and a representative carbonate electrolyte, specifically 1M $LiPF_6$ EC:DEC (1:1 by volume), through thermal and structural analyses. DSC is employed to evaluate the thermal reactivity of individual components and their combinations, highlighting the influence of each solvent and salt on the thermal reactivity and the TR-triggering reactions in LMBs at elevated temperatures. Complementary XRD analysis identifies the reactants and products formed during the chemical reactions between Li metal and the electrolyte. The results reveal that the melting of Li and the decomposition of $LiPF_6$ are key reactions responsible for triggering TR in LMB systems. Furthermore, the study demonstrates that the concentration of carbonate

Correspondence to: mt20@rice.edu

electrolytes plays a crucial role in determining the heat released during these reactions. These findings are crucial for addressing TR concerns and optimizing the design and performance of LMBs.

2 Experimental setup

Lithium and $LiPF_6$ were investigated as the metallic anode and salt, respectively, while the battery electrolyte solutions used in this study included ethylene carbonate (EC), diethyl carbonate (DEC), and their mixture EC:DEC (1:1, v:v). All sample preparation and storage were conducted in a glovebox to minimize the influence of O_2 and H_2O impurities. Thermal analysis was performed using a DSC 5+ instrument (Mettler Toledo). To prevent undesired reactions between samples and air, an argon flow of 50 mL/min was maintained throughout the experiments. The Li chips utilized in the experiments were standardized to a diameter of 1.5mm and a thickness of 100 μm, with an approximate weight of 0.095 mg to ensure consistent results. The total sample weight (Li+electrolyte) was around 5.0 ± 0.5 mg, except for experiments assessing the effects of electrolyte concentration. Samples were stored in 30-μL high-pressure stainless steel crucibles for 24 hours prior to DSC testing to ensure the complete formation of the SEI layer on the Li surface. Each sample was heated from 30℃ to 600℃ at a rate of 5 ℃/min. To ensure reproducibility, at least two independent tests were conducted for each sample.

The analyses were performed in strict accordance with the guidelines set forth by the International Confederation for Thermal Analysis and Calorimetry (ICTAC) Kinetics Committee to ensure the reliability of the experimental results [6]. The temperature accuracy and precision for the DSC were ± 0.2 K and ± 0.02 K, respectively. The power compensation mode with a short signal time (0.7 s) was set to obtain high-resolution results.

Structural characterization of the samples was identified by using X-ray diffraction (XRD) analysis. For these measurements, battery samples heated to 350℃ were utilized. XRD data were obtained using a Rigaku Smartlab II XRD system equipped with a semiconductor pixel array detector. Scans were conducted at a rate of 1º/min over the 2θ range of 10º to 90º at room temperature. The resulting crystalline structure patterns were compared against reference data from the Inorganic Crystal Structure Database (ISCD), the International Centre for Diffraction Data (ICDD), and Crystallography Open Database (COD).

3 Results

Figure 1 shows the thermal behaviors and reaction products of Li+EC and Li+DEC. Figure 1(a) illustrates that Li+EC underwent two exothermic reactions after the Li melting point. The first and the secondary reactions released -34.07 kJ/g Li and -12.62 kJ/g Li, respectively. The reaction products identified after the first exothermic reaction were EC, Li_2CO_3, and graphite, as shown in Fig. 1(b). Based on XRD results and previous research [7], two reaction pathways can be proposed, as described in Eq. (1) and (2). The theoretical heat of reaction for each reaction closely matches the experimentally measured values. However, $(CH_2OCO_2Li)_2$ was not detected in the XRD spectra, likely because it often forms as an amorphous product due to the rapid, non-equilibrium reaction conditions on the Li [8].

In contrast, for the Li+DEC reactions, exothermic reactions occurred before the Li melting point due to the SEI layer, which consists of ethyl lithium (C_2H_5Li) and $CH_3CH_2OCOOLi$ [9], both of which are highly soluble in carbonate solvents. The exothermic reaction released approximately -49.25 kJ/g of Li, as shown in Fig. 1(c). XRD results revealed that the primary reaction products included LiOH, Li_2CO_3, and LiC (Fig. 1(d)). Following this exothermic event, any remaining DEC undergoes boiling at around 169℃. Based on the thermodynamic characteristics and reaction products observed in the DSC and XRD tests, the most favorable chemical reaction between Li and DEC is described in Eq. (3). Additionally, any remaining $CH_3CH_2OCOOLi$ may subsequently decompose into LiOH, and C_2H_4, and CO_2, as shown in Eq. (4).

$$2Li + (CH_2O)_2CO \rightarrow Li_2CO_3 + C_2H_4,\ \Delta H = -34.6\ kJ/g\ of\ Li \quad (1)$$

$$2Li + 2(CH_2O)_2CO \rightarrow (CH_2OCO_2Li)_2 + 2C_2H_4,\ \Delta H = -12.10\ kJ/g\ of\ Li \quad (2)\ [\sim 6]$$

$$2Li + DEC \rightarrow Li_2CO_3 + C_2H_4 + C_2H_6,\ \Delta H = -43.99\ kJ/g\ Li \quad (3)$$

$$CH_3CH_2OCOOLi \rightarrow LiOH + C_2H_4 + CO_2 \quad (4)$$

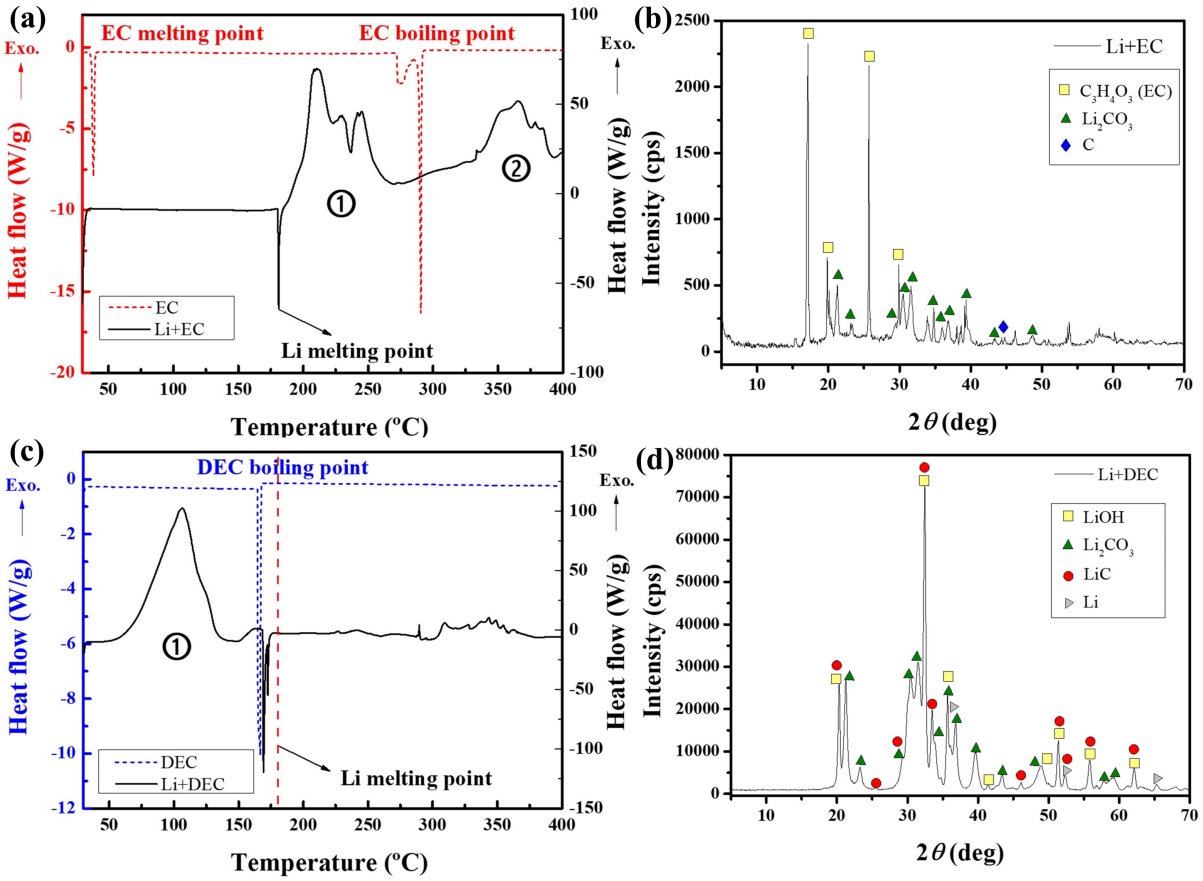

Figure 1: (a) DSC results of EC and Li+EC, (b) XRD pattern for Li+EC heated to 350°C, (c) DSC results of DEC and Li+DEC, and (d) XRD pattern for Li+DEC heated to 350°C.

Figure 2 presents the DSC thermograms and XRD spectra for Li-electrolytes without and with salt, respectively. Figure 2(a) shows that Li+EC:DEC (1:1) underwent similar exothermic reactions to Li+EC, indicating that the addition of DEC does not significantly alter the thermal behavior. This suggests that EC forms a stable SEI layer that effectively protects the Li metal from reacting with the carbonate electrolyte until Li melts. Regarding the reaction heat, Li+DEC released -49.30 kJ/g Li, while Li+EC released -34.07 kJ/g Li. For the Li+EC:DEC (1:1) mixture, the heat released was -40.49 kJ/g Li. When comparing this value to the average heat release of the Li+EC and Li+DEC systems (-41.69 kJ/g Li), the difference is only 3%, implying that the individual solvents in the mixture reacted independently with Li, without introducing intermediate reaction processes. Additionally, the secondary reaction for Li+EC:DEC (1:1) released -4.07 kJ/g Li, which can be attributed to the reduced EC content in the mixture.

Figure 2(b) displays the XRD patterns of the Li+EC:DEC (1:1) sample after heating to 250°C. Li_2CO_3 was identified as the primary reaction product formed from the Li+EC:DEC (1:1) system. Since Li+EC and Li+DEC reactions both yield Li_2CO_3 as a common product, these results strongly support the proposed chemical reaction mechanisms.

Figure 2(c) demonstrates that the onset temperature of the exothermic reaction is affected by the electrolyte composition, indicating that the strength of the SEI layer is impacted by the type of electrolyte used. For instance, Li+1M $LiPF_6$/EC showed a delayed and pronounced exothermic reaction at approximately 209°C, corresponding to the decomposition of $LiPF_6$. This delay reflects the stronger SEI layer formed by $LiPF_6$, which can also be disrupted upon $LiPF_6$ decomposition. The decomposition of $LiPF_6$ also generates the Lewis acid PF_5, which catalyzes the ring-opening and polymerization of EC as represented by Eq. (5). This reaction can release significant amounts of heat. In contrast, Li+1M $LiPF_6$/DEC exhibited an exothermic reaction at a relatively lower temperature, suggesting that the SEI layer formed in the DEC system remains weak despite the presence of $LiPF_6$. The thermal decomposition processes of $LiPF_6$+DEC can be summarized by Eqs. (6-11).

For Li+1M $LiPF_6$/EC:DEC (1:1), the onset temperature was not delayed to higher temperatures, likely due to the detrimental impact of DEC on the SEI layer quality. Additionally, this system exhibited a more rapid increase in heat flow at the onset of exothermic reactions compared to Li+EC:DEC (1:1). Regarding heat release, the primary exothermic reaction released around -59.98 kJ/g Li, while the secondary reaction released -15.04 kJ/g Li. In the Li+1M $LiPF_6$/EC:DEC (1:1) system, the primary exothermic heat exceeded the average value of -46.46 kJ/g Li, suggesting that the reaction between Li and 1M $LiPF_6$/EC is more favorable than that with Li and 1M $LiPF_6$/DEC. For the secondary reaction, the exothermic heat decreased to -15.04 kJ/g Li, likely due to the reduced proportion of EC in the mixture.

Figure 2(d) presents the XRD analysis of Li+1M $LiPF_6$/EC:DEC (1:1) after heating to 350°C. The major reaction product identified was LiF, with additional minor phases including $LiOH{\cdot}H_2O$, LiC, and $Li_4P_2O_7$. These crystal structures are consistent with the reaction products observed in both Li+1M $LiPF_6$/DEC and Li+1M $LiPF_6$/EC, confirming that both reaction pathways are likely to occur.

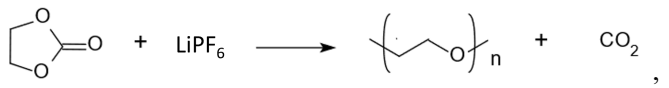

(5)

$\Delta H = -131.2$ kJ/g of Li (n=6)

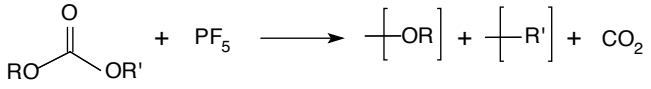

(6)

R and R' = $-CH_3$ or $-CH_2CH_3$

$$C_2H_5OCOOC_2H_5 + PF_5 \rightarrow C_2H_5OCOOPF_4 + HF + C_2H_4 \quad (7)$$

$$C_2H_5OCOOPF_4 \rightarrow OPF_3 + CO_2 + C_2H_4 + HF \quad (8)$$

$$LiOH + HF \rightarrow LiF + H_2O \quad (9)$$

$$Li_2O + 2HF \rightarrow 2LiF + H_2O \quad (10)$$

$$Li_2CO_3 + 2HF \rightarrow 2LiF + H_2CO_3 \quad (11)$$

To quantitatively evaluate the effect of electrolyte concentration on the thermal behavior of Li-electrolyte systems, the heat of reaction was plotted, as shown in Fig. 3(a). A linear increase in reaction heat was observed as the electrolyte-to-Li ratio (mol/mol) approached approximately 2.5, converging at around -66.64 kJ/g Li. This suggests that 1 mol of Li fully reacts with around 2.5 mol of 1M $LiPF_6$/EC:DEC (1:1), and any excess electrolyte does not significantly contribute to additional heat release. As shown in Fig. 3 (b), while the reaction between 1M $LiPF_6$ and EC generates a considerable amount of heat, $LiPF_6$ and DEC tend to react at lower temperatures. Additionally, EC and DEC may undergo reactions with each other at elevated temperatures. Due to the complexity of the reaction process, the heat of reaction does not follow a simple dependence on the electrolyte quantity.

To mitigate the thermal reactivity between Li and carbonate electrolytes at elevated temperatures, it is essential to prevent the reaction between $LiPF_6$ and EC. DSC tests for 1M $LiPF_6$/FEC were conducted to determine whether FEC undergoes ring-opening and polymerization like EC. As shown in Fig. 3(c),

FEC exhibited only endothermic reactions, suggesting that FEC could be a viable alternative to EC in carbonate-based electrolytes.

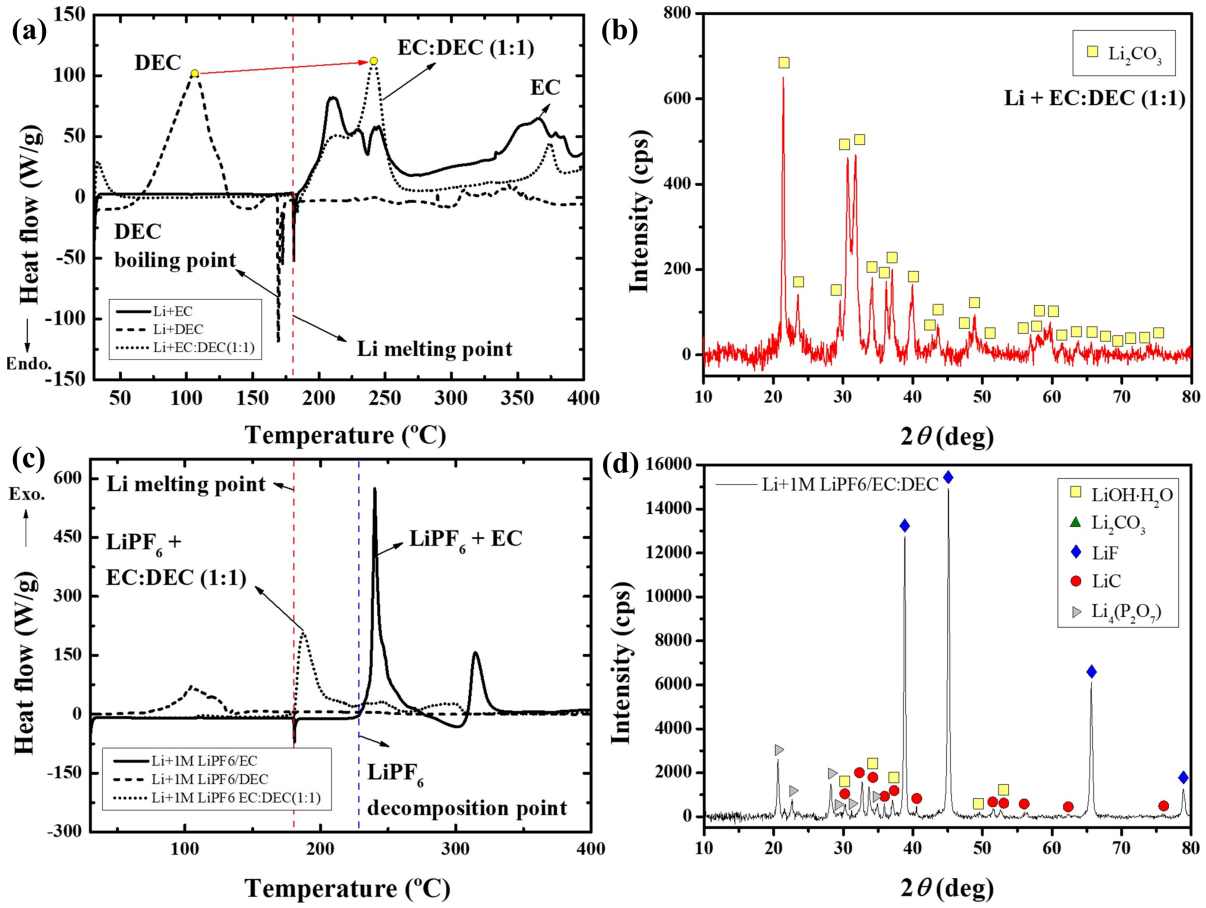

Figure 2: (a) DSC results of Li-electrolytes without $LiPF_6$, (b) XRD pattern for Li+EC:DEC (1:1) heated to 350°C, (c) DSC results of Li-electrolytes with $LiPF_6$, and (d) XRD pattern for Li+1M $LiPF_6$/EC:DEC (1:1) heated to 350°C.

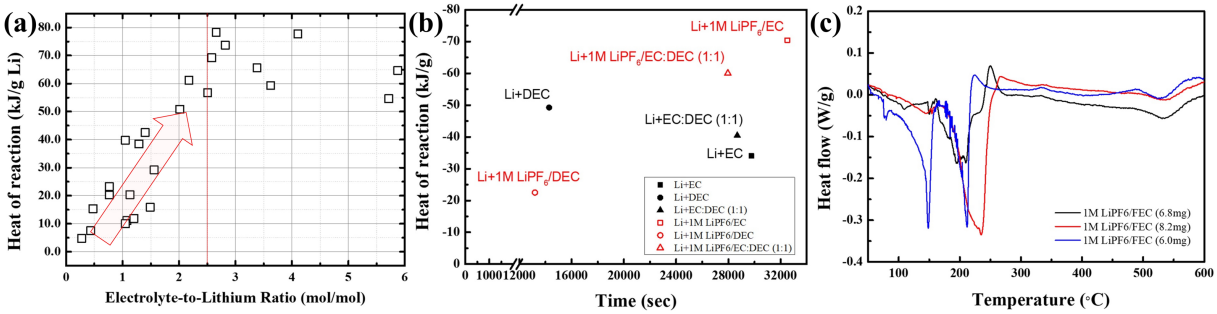

Figure 3: (a) Effect of electrolyte concentration on the heat of reaction in Li-electrolyte systems, (b) Variation of the heat of reaction on time, and (c) DSC results for 1M $LiPF_6$/FEC at 5°C/min.

4 Conclusion

The present study has systematically investigated the thermal behaviors and structural characteristics of Li-1M $LiPF_6$/EC:DEC (1:1) electrolyte systems. It was found that the exothermic reaction of the Li-EC system was initiated right after Li melting, producing Li_2CO_3 and C_2H_4. In contrast, the Li-DEC system

exhibited reactions before Li melting, attributed to the soluble SEI layer. For the Li-EC:DEC system, the reaction began after Li melting, primarily due to the solid SEI layer formed by EC. Also, each solvent reacted independently with Li, contributing to the overall heat release in parallel.

The presence of $LiPF_6$ significantly influenced the thermal behavior of these systems. In the Li-1M $LiPF_6$/EC system, exothermic reactions were delayed due to a strengthened SEI layer. $LiPF_6$ leads to a notable heat release by catalyzing the EC-ring opening and polymerization through the generation of PF_5. On the other hand, the thermal behavior of Li-1M $LiPF_6$/DEC remained similar to the Li-DEC system. For the Li-1M $LiPF_6$/EC:DEC (1:1) system, it was identified that the reaction between Li and 1M $LiPF_6$/EC was more energetically favorable compared to the other systems.

The study has identified Li melting and $LiPF_6$ decomposition as the primary triggers of TR in Li-electrolyte systems, as these reactions disrupt the SEI layer, leading to EC ring-opening and polymerization, a major source of heat release. As a strategy to mitigate the probability of TR, FEC emerges as a viable alternative to EC, as it successfully prevents the EC ring-opening and polymerization. Overall, this work provides valuable insights into the reaction pathways responsible for TR in Li-carbonate electrolyte systems. The findings highlight critical factors that govern the thermal reactivity of LIB systems and suggest potential mitigation strategies.

References

[1] Ding JF, Zhang YT, Xu R, Zhang R, Xiao Y, Zhang S, Bi CX, Tang C, Xiang R, Park HS, Zhang Q. (2023). Review on lithium metal anodes towards high energy density batteries. Green Energy & Environment, 8: 1509.

[2] Wang J, Ge B, Li H, Yang M, Wang J, Liu D, Fernandez C, Chen X, Peng Q. (2021). Challenges and progresses of lithium-metal batteries. Chemical Engineering Journal, 420: 129739.

[3] Lu B, Cheng D, Sreenarayanan B, Li W, Bhamwala B, Bao W, Meng YS. (2023). Key parameters in determining the reactivity of lithium metal battery. ACS Energy Letters, 8: 3230.

[4] Puthusseri, D., Parmananda, M., Mukherjee, P.P. and Pol, V.G., 2020. Probing the thermal safety of Li metal batteries. *Journal of The Electrochemical Society*, *167*(12), p.120513.

[5] Jiang, F.N., Cheng, X.B., Yang, S.J., Xie, J., Yuan, H., Liu, L., Huang, J.Q. and Zhang, Q., 2023. Thermoresponsive electrolytes for safe lithium-metal batteries. Advanced Materials, 35(12), p.2209114.

[6] S. Vyazovkin, K. Chrissafis, M.L.D. Lorenzo, N. Koga, M. Pijolat, B. Roduit, N. Sbirrazzuoli, J.J. Suñol, ICTAC Kinetics Committee recommendations for collecting experimental thermal analysis data for kinetic computations, Thermochim. Acta 590 (2014) 1-23.

[7] LaFollette, Rodney, and Michael D. Eskra. "Lithium Ion Battery Failures and the Formation of Thermite Reactions."

[8] Wang, L., Menakath, A., Han, F., Wang, Y., Zavalij, P.Y., Gaskell, K.J., Borodin, O., Iuga, D., Brown, S.P., Wang, C. and Xu, K., 2019. Identifying the components of the solid–electrolyte interphase in Li-ion batteries. Nature chemistry, 11(9), pp.789-796.

[9] M. He, L. Boulet-Roblin, P. Borel, C. Tessier, P. Novak, C. Villevieille, and E. J. Berg, ´ J. Electrochem. Soc., 163, A83 (2016).